Study of FBG-based optical sensors for thermal measurements in aerospace applications

Study of FBG-based optical sensors for thermal measurements in aerospace applications

To cite this article: A. Aimasso *et al* 2022 *J. Phys.: Conf. Ser.* **2293** 012006

Study of FBG-based optical sensors for thermal measurements in aerospace applications

A. Aimasso, M.D.L. Dalla Vedova, P. Maggiore and G. Quattrocchi

Dept. of Mechanical and Aerospace Engineering, Politecnico di Torino, Torino, Italy

E-mail: alessandro.aimasso@studenti.polito.it, matteo.dallavedova@polito.it

Abstract. Optical fibers have revolutionized several technological sectors in recent decades, above all that of communication, and have also found many applications in the medical, lighting engineering, and infrastructural fields. In the aerospace field, many studies investigated the adoption of fiber optics considering the planned transition from fly-by-wire to fly-by-light flight controls. A significant feature of optical fiber is its ability to be used not only as a transmission medium but also as a basis for fiber-embedded sensors; one of the most prominent types is based on Bragg gratings (FBGs). FBGs can replace several traditional sensors, providing measures of temperature, vibrations, and mechanical deformation. Optical sensors provide many advantages over traditional, electrical-based sensors, including EMI insensitivity, ease of multiplexing on a single line, resilience to harsh environments, very compact sizes and global weight saving. Furthermore, punctual knowledge of the temperature field is essential to perform the thermal compensation of the optical sensors used for strain measurements. In this work, the authors analyzed the performance of thermal sensors based on FBGs to verify their stability, accuracy, and sensitivity to operating conditions. Two different methods of FBGs surface application have been considered (gluing with pre-tensioning vs. non-tensioned bonding). The results were then compared to those acquired using typical temperature sensors to determine the relationship between the observed temperature and the Bragg wavelength variation (i.e. the proportionality coefficient Kt). The effects on the proportionality coefficient Kt, arising from fiber pre-tensioning and thermal expansion of the structural support, were then evaluated by comparing the results obtained with the two bonding approaches.

1. Introduction

The optical fiber is a material composed by a glass cylindric structure which is able to conduct light into itself. Because of this unique characteristic, the usage of fiber has risen in recent decades, particularly with applications in a wide variety of industrial sectors such as communications, medical diagnostics, lighting, the Internet, and many others. Currently, optical fiber is a core technology that is steadily used in everyday applications, and it has established a wide spread throughout the global economy. Nowadays, the most well-known application of optical fiber is the development of particular connections to provide increasingly efficient communications and quicker Internet surfing speed. But thanks to some specific characteristics of this material, the use of the optical fiber has been resulted strategic also for the aerospace sector. Moreover, it could also be employed in sensor applications, thanks to the possibility of creating specific structures inside the fiber which act as a sensor, such as the case of *Fiber Bragg Gratings* (FBG) [1-7].

Journal of Physics: Conference Series **2293** (2022) 012006 doi:10.1088/1742-6596/2293/1/012006

In modern engineering projects and researches, an important role is played by the new types of sensors combining high performance (in terms of sensibility, accuracy, and reliability) with a marked resilience to external disturbances (e.g., EM noise or electrostatic discharges) and other environmental factors [8-9]: FBG sensors, suitable for measuring various engineering parameters in both static and dynamic modes, meet all these requirements [10-11]. In aerospace, they could replace traditional sensors [12], not only in structural monitoring [13] but also in vibration measurements [14-15], pressure sensors [16], and thermal control and compensation [17-19].
Their resistance to electromagnetic interference, combined with a wide operating temperature range and weight gain, make them ideal for space applications.
Aim of this work is to analyze the performance of thermal sensors based on FBGs to verify their stability, accuracy, and sensitivity to operating conditions, in particular by comparing two different methods of their fixing (gluing with pre-tensioning vs. non-tensioned bonding). The experimental test on the fiber was possible thanks the collaboration with PhotoNext, the competence center on Photonics launched by POLITO in summer 2017 [20].

2. Optical fiber and FBG sensors

2.1. About optical fiber structure

As already described in the introduction, the optical fiber has got the capacity of conducing light inside itself. It presents a cylindrical structure with several concentric layers: the core, the cladding, and the coating.
The core represents the most internal part and it lets the passage of the desired information, in terms of light signal. It is typically composed by glass or a polymeric material and it usually reaches a thickness of at most 50 μm.
The cladding is the intermediate layer and it is necessary to guarantee the correct operation of the entire optical fiber. Generally, it reaches a diameter of 125 μm.
The coating is the external layer and it is placed to protect the structure from eventual damages, because the fiber has got a really low bending resistance. Due to its extreme fragility, some additional external layers could be added to improve the mechanical strength.
The physical principle at the base of the signal propagation into the fiber is the Snell's law:

$$\boldsymbol{n_1 sen(\theta_1) = n_2 sen(\theta_2)} \tag{1}$$

where n_1 is the refraction index of material 1, n_2 is the refraction index of material 2, θ_1 is the incidence angle, θ_2 is the refraction angle.
If the light beam is introduced in the core with an appropriate orientation, when it reaches the interface with the cladding, it will undergo a total reflection, so resulting confined within the optical fiber, allowing in this way the signal transmission. The maximum allowed angle for the light to enter in the fiber is calculated as:

$$\boldsymbol{\alpha_{\max} = arcsen\left(\frac{\sqrt{(n_1^2 - n_2^2)}}{n_0}\right)} \tag{2}$$

Where n_0 is the refractive index of the environment from the light comes.

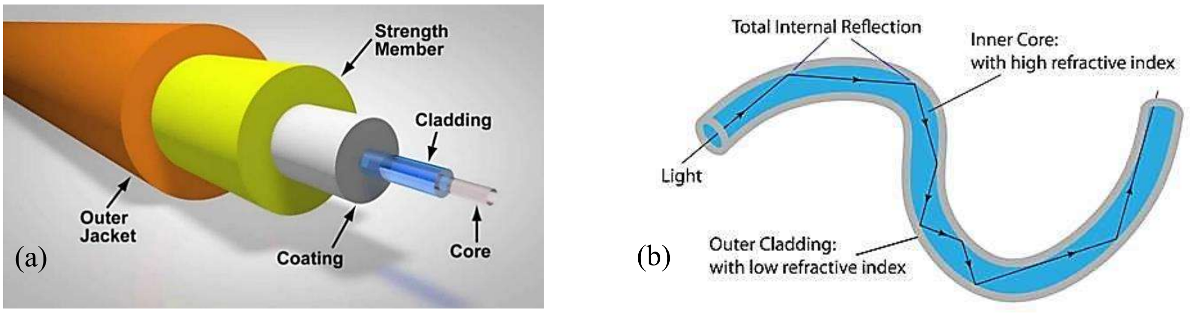

Figure 1. *The optical fiber structure (a) and the signal propagation mechanism (b)*

2.2. About FBG working principles

The sensors used for our tests are spectral modulation type called *Fiber Bragg Gratings* (FBG). They are built in the fiber itself thanks to a periodical variation of the core refractive index using a laser technique. At the end of this process, in a trait of fiber of about 1 cm, there are some bands of the core with a new refractive index, which results $n_f = n_i + \Delta n$. Each of the parties with the modified refractive index are placed at a specific distance, which is called *grating period* Λ_G.
This process makes the sensor able to act like a filter: indeed, when the light crosses through it, the FBG reflects a certain wavelength, called *Bragg frequency*, following the equation:

$$\lambda_B = 2n_{EFF}\Lambda_G \tag{3}$$

where λ_B is the wavelength reflected by the FBG, n_{EFF} is the refractive index of the fiber (after the remodulation), Λ_G is the pitch of the grating as shown in figure 2. The Bragg frequency represents the output of the sensor.

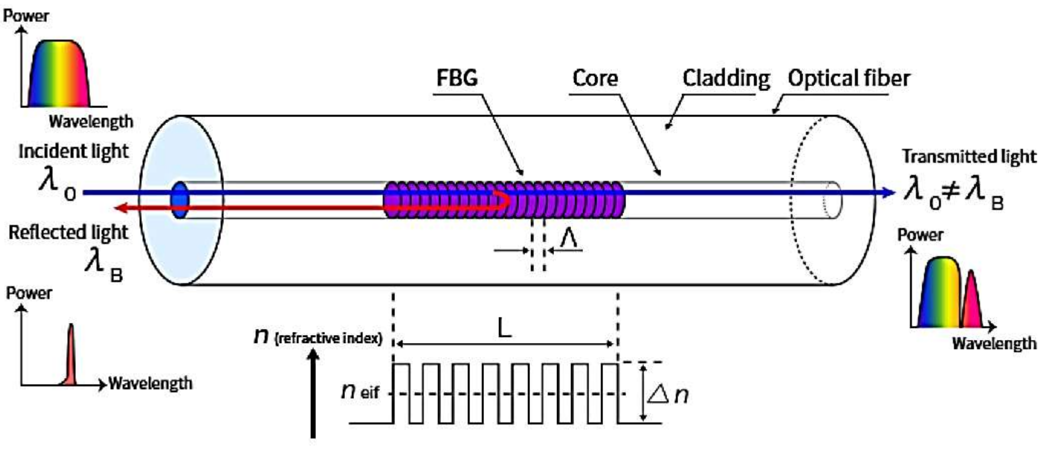

Figure 2. *FBG working mechanism*

The equation 3 reveals the Bragg frequency's dependence on the grating pitch, which is a physical distance: this means that the reflected wavelength's variation is always associated to a mechanical strain induced on the grating period by an external factor. Therefore, it is easy to understand that loads applied on the sensor (in terms of induced strain) or thermal excursion cause a significative variation on the FBG's reflected wavelength, and consequently the equation 3 could be written in the following form:

$$\Delta\lambda_B = K_\varepsilon\Delta\varepsilon + K_T\Delta T \tag{4}$$

3. The test bench developed for the tests

Thanks to the results gained during several FBG test campaigns conducted over the years, this time we have developed an experimental bench specifically designed for fiber's thermal calibration. As shown in figure 3, it consists of three main subsystems (called "Fridge," "Table," and "Radiator"), each of which is expressly designed to test the sensors in three different operating scenarios (to evaluate three scenarios with different time histories of environmental conditions) and study the response of FBGs to variable temperature and relative humidity. The test bench's primary components are as follows:

- Three optical fibers with related FBG sensors;
- Mechanical fiber support frames;
- FBG Interrogator;
- Electrical power unit;
- SHT85 temperature and humidity sensors;
- ARDUINO UNO microcontroller;
- Personal computer (PC).

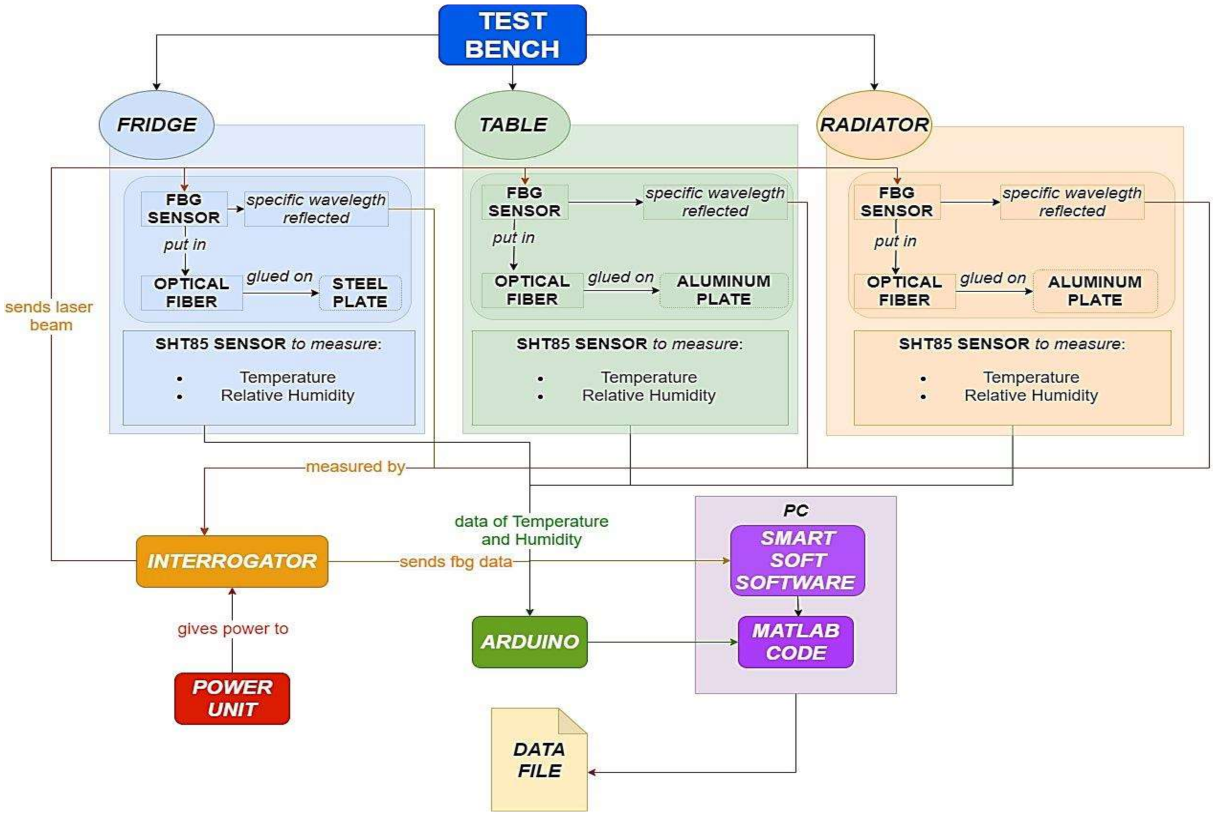

Figure 3. *Scheme of the developed test bench*

More in detail, the FBG *Interrogator* is a device capable of automatically recognizing and questioning the FBGs in the fibers connected to the various channels, as well as collecting and analyzing their replies. It provides a distinct communication channel for each FBG, preventing potential misunderstandings about data from various sensors. The interrogator sends a laser beam through the fiber and measures the reflected wavelengths. A SmartScan SBI laser interrogator produced by the Smart Fibres society was employed in this application [21]. The system operates a data acquisition loop one time per minute: each one has a duration of 1 seconds with a sampling frequency of 25 kHz. All data acquired in a specific measurement on a given Bragg are averaged, obtaining the related instantaneous wavelength value.

Each FBG is accompanied with a *SHT85* sensor, which measures the local temperature and humidity at the same time (thus providing an indication of the actual conditions to which the FBGs are subjected). This sensor has an operational temperature range of -40 to +105 °C and measures relative humidity levels ranging from 0% to 100%. These sensors have been programmed to collect temperature and relative humidity measurements for the same time interval as the Smart Scan.
The *ARDUINO UNO microcontroller* is the electronic board which shall receive and communicate data acquired by SHT85 sensors. It sends information about sensors to the personal computer (PC) by using a USB link. These data are saved using a python code. Finally, the overall post-processing analysis is made with a MATLAB script.

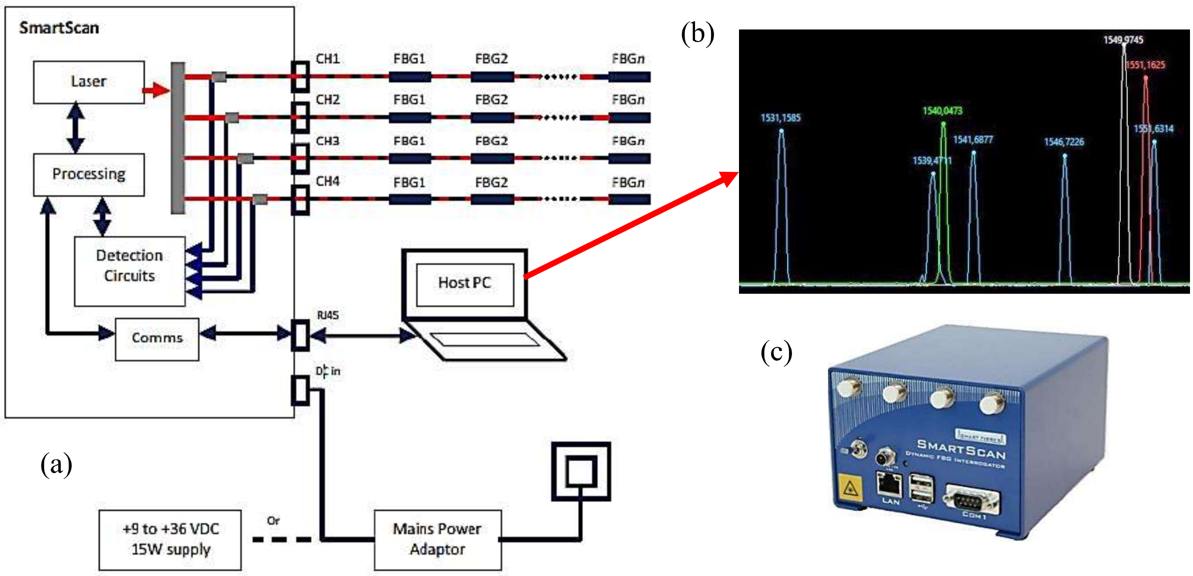

Figure 4. *Scheme of Interrogator's working mechanism (a), example of graphical interface (b) and the Smart Scan used (c)*

For the current work, we focused our efforts on the measurement station put near the radiator. We used two fibers near our heat source: a first fiber was pre-tensioned and glued on the metal support with an epoxide resin, while a second fiber was only adhered to the metal plates with a simple adhesive.

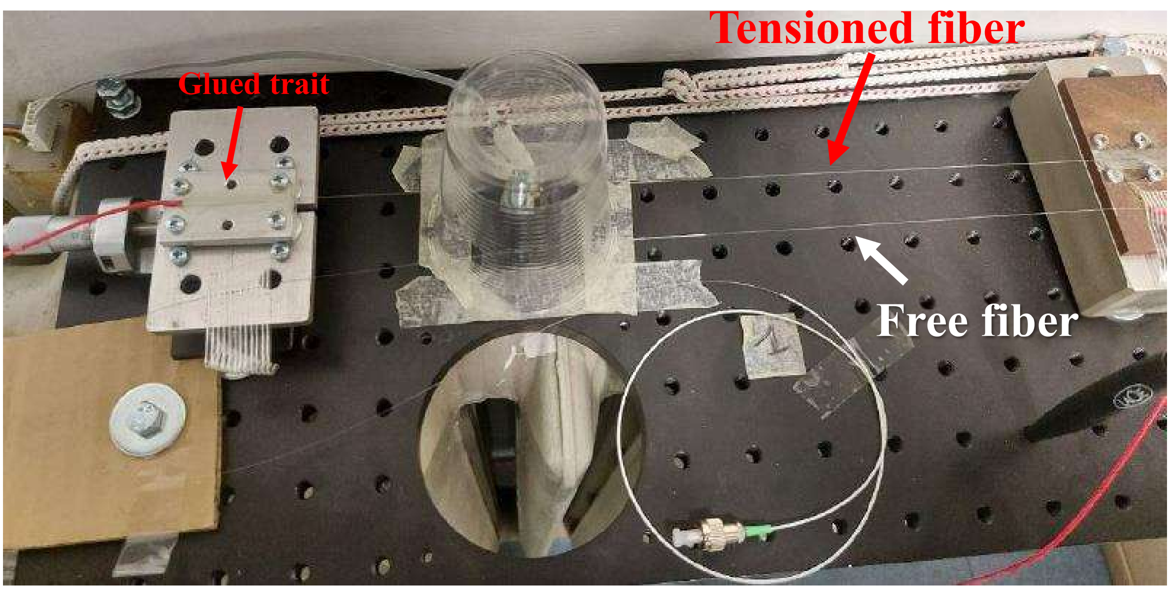

Figure 5. *The two fibers employed in this study*

4. Experimental tests

The experimental campaign covered numerous measurement cycles on the two fibers under consideration, one subjected to pre-tensioning and the other simply fixed on the metal support. Each measurement cycle included the possibility of varying the environmental temperature by altering the heat supplied by the radiator. In this manner, the mathematical correlation between temperature and wavelength trends was first seen and then quantified. This association appears to be the foundation for verifying this technology's usage as a temperature sensor.

4.1. About row data acquired

The total amount of data supplied derive from numerous measurement cycles, each with a specific detection period and temperature excursion range. Temperature and FBG wavelength qualitative trends demonstrate a strong correlation between these two parameters. Furthermore, when compared to the free fiber, the Δλ observed in the pretensioned fiber has got a greater amplitude. Finally, always considering the tensioned fiber, the FBG output appears more stable, with a very low noise to signal ratio.

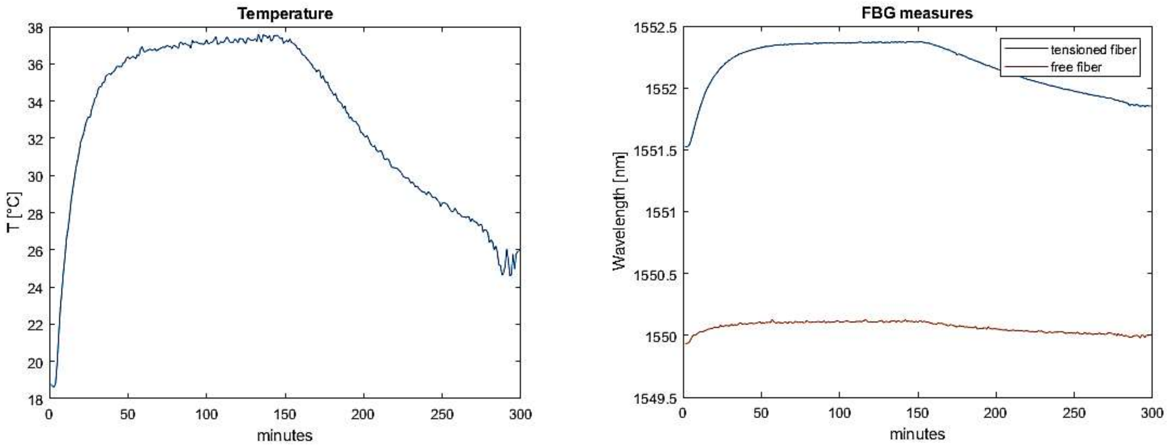

Figure 6. *The temperature and FBGs trends during the test*

4.2. About data management

Aim of the post-processing analysis carried out in this work is to quantify the correlation between the ΔT measured by the SHT85 sensor and the Δλ of the FBG detected by the Smart Scan.
At first, we consider the general equation of an FBG:

$$\Delta\lambda = K_T \Delta T + K_\varepsilon \Delta_\varepsilon \qquad (5)$$

When the fiber and its structural support do not undergo some mechanical stress, each FBG wavelength value corresponds to a specific environmental temperature. For this reason, studying the available data, three temperature steps were taken into account for each measurement cycle, along with the associated wavelength value. A linear correlation between the two parameters was observed: thus, the three steps, once collocated on the *T*-λ plane (figure 7), allowed us to calculate the equations of the three straight lines passing through the three points (which are considered two by two) in the form:

$$\lambda(T) = \lambda_0 + K_T T \qquad (6)$$

As a result, 102 values for the coefficients λ_0 and K_T were found for both free and tensioned fiber.

Because of the large number of available data, the median and average values were calculated for all the coefficients, and then employed in the generic equation. This could be applied for all the measurement cycles.

$$\lambda(T) = \lambda_{0_{mean}} + K_{T_{mean}} T \tag{7}$$

Finally, after computing the mean and median values – reported in table 1 – we verified that they fall within the most frequent interval of experimental data obtained. This was validated, as indicated in the figure 8, and the average of value for each coefficient may now be assumed to transform the FBG output into a temperature measurement. Indeed, from equation 7 it is immediate to obtain:

$$T(t) = \frac{\lambda(t) - \lambda_{0_{mean}}}{K_{T_{mean}}} \tag{8}$$

This procedure is carried out for both tensioned and free fiber.

Table 1. *Coefficients obtained after the data interpolation*

Coefficient	Mean value		Median Value	
	Free	Tensioned	Free fiber	Tensioned
K_T	0.0100	0.0449	0.0089	0.0458
λ_0	1549.7	1550.7	1549.8	1550.7

4.3. Results and discussion

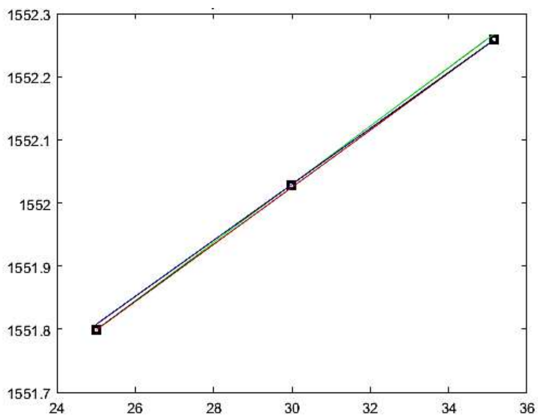

Figure 7. *An example of interpolation in T-λ plane*

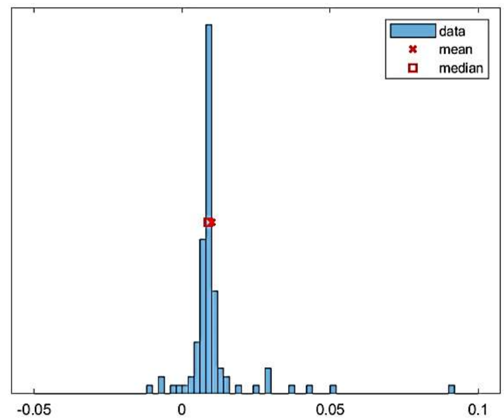

Figure 8. *Example of histogram of most frequent data intervals*

The above-mentioned post-processing study quantified a linear relationship between the wavelength reflected by the FBG sensor and the temperature. As a result, optical technology can be used as a temperature sensor in mechanically stable situations. The values acquired were utilized to translate the data coming from the fibers into temperature, and the resulting trends were compared to how detected by typical electronic sensors. The coefficients K_T found on the two FBGs (although having the same nominal Bragg frequency) are different, as shown by table 1: this is not surprising given that one of the two fibers was pre-tensioned. Precisely, the applied tension appears to have a significant influence on the results achieved: figure 9 depict the application throughout two separate testing cycles, which have been purposefully different to investigate sensors sensitivity to low and medium temperature ranges.

The first phase (shorter) consists of a single rise with a ΔT of around 20 °C, followed by a stationary period, with finally a drop to nearly beginning values (but with a different slope from the ascent). The second, on the other hand, is divided into a much longer period with a 20 °C descent, an intermediate phase with repeated ups and downs with a ΔT of about 5 °C, and finally a 20 °C rise.
The graphics show how the pre-tensioned fiber's trend is more stable. This is because the pre-tensioning causes a significantly larger wavelength excursion than the free fiber, and as a result, any perturbations in the measurement (caused for example by small random mechanical phenomena) appear to be almost insignificant. In fact, the amplitude of the disturbance on the signal is about the same in both circumstances, but in the tensioned fiber, this relates to an overall $\Delta\lambda$ that is nearly an order of magnitude higher, rendering these oscillations practically inconsequential.
Moreover, we can deduce an exceptional sensitivity of the fiber to the environmental circumstances to which it is subjected, and in particular, a significant sensitivity to mechanical disturbances, which, if not effectively filtered, might lead to very incorrect thermal calculations. In addition, the two measurement cycles depicted in the graphs below are a practical proof of what has just been stated: in the first example, considerable oscillations of the free fiber curve around the real temperature are observed and these oscillations are attributable to the motion of the convective flow of the heated air from the radiator. In the second case, instead, the curve shifts upwards in addition to the previous oscillations. The error is probably due to the mechanical effect of the weight force acting on the fiber, which is suspended between the two metal supports: in the absence of pre-tensioning, the self-induced stress by the weight of the fiber is significant, unlike the previous case.
The overall average error for the equivalent measured temperature then resulted more consistent in the free fiber and equal to about 4%; at contrary for the pre-tensioned one it resulted about the 1,1%.

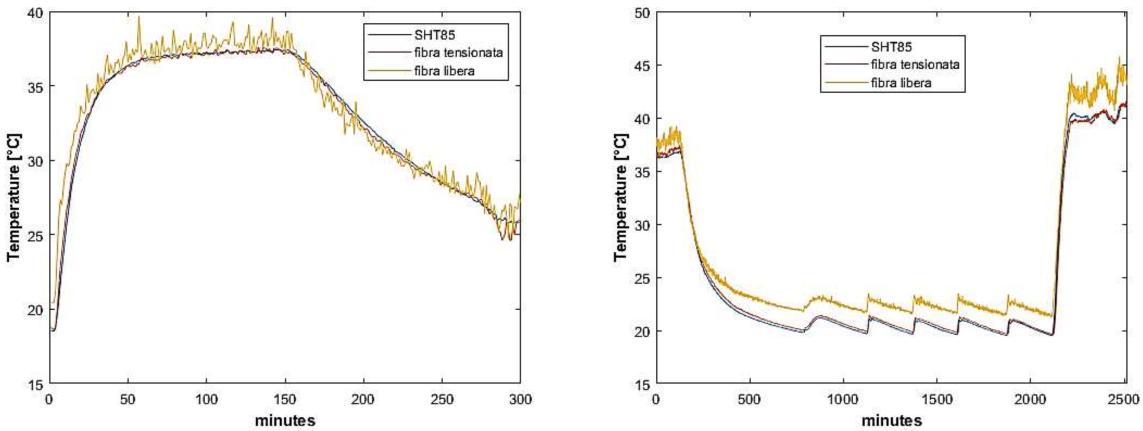

Figure 9. *Two examples of comparison between temperature measure by SHT85 sensor, FBG in tensioned fiber and FBG in free fiber*

5. Conclusions

The experiment produced extremely positive and encouraging results. At first, the correlation between the output of the FBG sensors and the temperature was demonstrated and quantified, validating these sensors for temperature detection. From the comparison of the two different solutions, we observed that the pre-tensioned fiber has higher accuracy values than the free fiber, which has larger errors. Moreover, this study confirms the high fiber's sensitivity to environmental conditions and, more broadly, to mechanical stresses, even random ones, to which it might be subjected. If these effects are not properly assessed, they can generate unacceptable amplifications of the measurement error.
As a result of this test campaign, it is possible to conclude that a pre-tensioned fiber bonded to a metal support is more accurate than a free and simply fixed fiber. The results, however, show that the proportionality between wavelength and temperature varies with the applied tension on the fiber.

Journal of Physics: Conference Series **2293** (2022) 012006 doi:10.1088/1742-6596/2293/1/012006

The correlation that characterize the free fiber appears to be more standardizable compared to how calculated for the tensioned one, where a calibration that takes the tension into account is required for every application. Finally, it can be inferred that the pre-tensioned optical fiber could be more advantageous for highly accurate temperature readings and in the presence of law thermal excursions with potentially disturbing effects (such as convective air motions). Instead, in the presence of severe temperature excursions and/or relatively steady circumstances, even free fiber could provide good performances. In this regard, free fiber appears to be particularly suited for space applications.
Further testing campaigns, conducted by altering the materials employed and increasing the temperature range to which the specimens will be subjected, may offer more information on the usage of FBGs as temperature sensors for aerospace applications.

References

[1] Mihailov S J 2012 Fiber Bragg grating sensors for harsh environments *Sensors* **12(2)** 1898–1918
[2] Mihailov S J, Grobnic D, Hnatovsky C, Walker R B, Lu P, Coulas D and Ding, H 2017 Extreme Environment Sensing Using Femtosecond Laser-Inscribed Fiber Bragg Gratings *MDPI Sensors* **17(12)** 2909
[3] Habel J, Boilard T, Frenière J S, Trépanier F and Bernier M 2017 Femtosecond FBG written through the coating for sensing applications *MDPI Sensors* **17(11)**, 2519
[4] Grobnic D, Mihailov S, Smelser C W and Ding H 2004 Sapphire Fiber Bragg Grating Sensor Made Using Femtosecond Laser Radiation for Ultrahigh Temperature Applications *IEEE Photonics Technology Letters* **16(11)**, 2505–2507
[5] Santos J L and Farahi F 2018 *Handbook of Optical Sensors* CRC Press
[6] Ahuja D and Parande D 2012 Optical sensors and their applications *J. Sci. Res. Rev.* **1(5)**, 60–8
[7] Giurgiuntiu V 2016 Structural health monitoring of aerospace composites *Fiber-Optic Sensors*
[8] Kersey A D 1996 A review of recent developments in fiber optic sensor technology *Optical Fiber Technology* 291–317
[9] Xin G, Zhengying L, Fan W, Yiming W, Changjia W, Siyue Z and Haihu Y 2017 *Optics Express* **25**, 28112
[10] Berri P C, Dalla Vedova M D L, Maggiore P and Scolpito T 2019 Feasibility study of FBG-based sensors for prognostics in aerospace applications *Journal of Physics: Conference Series* **1249**, 012015
[11] Dalla Vedova M D L, Berri P C, Maggiore P and Quattrocchi G 2020 Design and development of innovative fbg-based fiber optic sensors for aerospace applications *Journal of Physics: Conference Series* **1589**, 012012
[12] Tanaka N, Okabe Y and Takeda N 2003 Temperature-compensated strain measurement using fiber Bragg gratings sensors embedded in composite laminates *Smart Materials and Structures* **12(6)**, 940–946
[13] Brusa E, Dalla Vedova M D L, Giorio L and Maggiore P 2021 Thermal condition monitoring of large smart bearing through fiber optic sensors *Mechanics of Advanced Materials and Structures* **28(11)** 1187–1193
[14] Quattrocchi G, Berri P C, Dalla Vedova M D L and Maggiore P 2021 Optical fibers applied to aerospace systems prognostics: design and development of new FBG-based vibration sensors *IOP Conference Series: Materials Science and Engineering* **1024**, 012095
[15] Dalla Vedova M D L, Quattrocchi G, Berri P C and Maggiore P 2021 Preliminary Analysis on Environmental and Intrinsic Factors on FBG-Based Vibration Sensors *Journal of Physics: Conference Series* **1977(1)**, 012011
[16] Liu L, Zhang H, Zhao Q, Liu Y and Li F 2007 *Optical fiber technology* **13**, 78–80
[17] Kisala P and Cieszczyk S 2015 *Applied Optics* **54**, 2677–2687
[18] Wenyuan W, Yongqin Y, Youfu G and Xuejin L 2015 Measurements of thermo-optic coefficient of standard single mode fiber in large temperature range *Proc. Int. Conf. Optical Instr. and Tech.: Optical Sensors and applications*, 9620

[19] Berri P C, Dalla Vedova M D L, Maggiore P and Secci C 2020 Fiber Bragg gratings for prognostics in space applications: a thermo-mechanical characterization of minimally invasive sensing techniques *Proc. 1st Aerospace Europe Conference AEC 2020* (Bordeaux)
[20] https://www.photonext.polito.it/
[21] Aimasso A 2020 Study and analysis of FBG sensors for aerospace applications, *MSc Thesis*, https://webthesis.biblio.polito.it/view/creators/Aimasso=3AAlessandro=3A=3A.html